Journal of Zhejiang University SCIENCE A
ISSN 1673-565X (Print); ISSN 1862-1775 (Online)
www.zju.edu.cn/jzus; www.springerlink.com
E-mail: jzus@zju.edu.cn

Mixed nonlinear dynamic voltage phasor tracing method based on WAMS/SCADA*

Xiao-gang CHEN[1,2], Yong-hui YI[1], Wei WANG[3], Quan-yuan JIANG[†‡1], Chuang-xin GUO[1], Yi-jia CAO[1]

([1]*School of Electrical Engineering, Zhejiang University, Hangzhou 310027, China*)

([2]*Hangzhou Electric Power Bureau, Hangzhou 310009, China*)

([3]*Zhejiang Provincial Electric Power Company, Hangzhou 310007, China*)

[†]E-mail: jqy@zju.edu.cn

Received Mar. 4, 2008; Revision accepted July 8, 2008; Crosschecked Apr. 10, 2009; Published online May 2, 2009

Abstract: By considering the static voltage characteristic of the load, we propose a WAMS/SCADA mixed nonlinear method to estimate the voltage of unobservable buses caused by topology change or phasor measurement unit (PMU) malfunction in a power system. By modeling the load characteristic with data from SCADA, we employed the Gauss-Seidel method to solve the nonlinear equations and estimate the voltage of unobservable buses with the high precision voltages of neighboring buses measured by a PMU. Simulations were carried out on the IEEE 39-bus system, and the results show that this novel method can dynamically and accurately trace the variation of the voltage phasor of the unobservable buses.

Key words: Wide area measurement system (WAMS), Supervisory control and data acquisition (SCADA) system, Observability, Dynamic tracing, Nonlinear equation

doi:10.1631/jzus.A0820150 **Document code:** A **CLC number:** TM734

INTRODUCTION

Power outages over large geographical regions dramatically affect the power system reliabilities, interrupt the electric supply to residential, commercial, and industrial users, and result in tremendous loss on millions of customers. As the power grid increases in both size and complexity, it becomes more important to monitor and control the heavy loaded power grid by an advanced information system with higher accuracy and faster speed (Zima *et al.*, 2003; Quintero and Venkatasubramanian, 2005; Chen and Abur, 2006).

A supervisory control and data acquisition (SCADA) system is a power grid monitoring system at present time, but cannot trace the dynamic information of the power system. The fast developing wide area measurement system (WAMS), constituted of phasor measurement units (PMUs), can supply dispatchers with real time and accurate dynamic voltage phasor information (Quintero and Venkatasubramanian, 2005). So far, many experts and scholars have researched WAMS to reduce the probability of a large blackout in a power system (Huang *et al*., 2002; Rehtanz and Bertsch, 2002; Chaudhuri *et al*., 2004; Okou *et al*., 2005). But the precondition of this advanced technology is that the power grid should be fully observable. In comparison with the traditional SCADA system, the measurement redundancy of WAMS is much lower, which makes it easier than SCADA to lose its full observability in case of cascading failures and PMU malfunction. Once the full observability is lost, the linear state estimation cannot

‡ Corresponding author

* Project supported by the National Natural Science Foundation of China (Nos. 50507018, 50595414, 50677062, and 60421002), the National Basic Research Program (973) of China (No. 2004CB217902), the National Key Technologies Supporting Program of China during the 11th Five-Year Plan Period (No. 2006BAA02A01), and the Key Grant Project of MOE of China (No. 305008)

run properly due to the singularity in matrix inversion.

As a result, proper countermeasures must be taken to restore the full observability of WAMS the moment the full observability is lost. Reynaldo (2001) proposed a linear estimation of voltages on unobservable buses with neighboring measured voltages by PMUs, which can observe the voltage of an unobservable bus dynamically. But the accuracy will deteriorate notably if the system suffers large disturbances due to its ignorance of both the voltage characteristics of the load and the susceptance of the transmission line.

This paper proposes a countermeasure to restore the observability of WAMS. The Gauss-Seidel method was used to solve the nonlinear equations and estimate the unobservable bus voltages with high precision neighboring bus voltages measured by PMUs. Simulation results justify the accuracy and efficiency of this new method.

VULNERABILITY OF WAMS TO CASCADING FAILURES AND PMU MALFUNCTION

In this section, we will first briefly introduce the concept of 'observability', and then analyze the impact of cascading failures and PMU malfunction on the observability of WAMS.

Full observability of WAMS

The state estimation is based on the relationship between the values measured within the system and the unknown state variables, as shown in Eq.(1):

$$\boldsymbol{Z}^{\text{meas}}=\boldsymbol{H}\cdot\boldsymbol{x}+\boldsymbol{\varepsilon}, \tag{1}$$

where $\boldsymbol{Z}^{\text{meas}}$ is the column vector of measured values, $\boldsymbol{H}$ is the matrix of coefficients relating to the known and unknown variables based on system topology, $\boldsymbol{x}$ is the column vector of estimated voltages, and $\boldsymbol{\varepsilon}$ is the column vector of measurement errors.

In order to account for a system where there are more measured values than unknown values, it is helpful to construct an expression that gives the maximum likelihood of the unknown values through a weighted least squares (WLS) calculation of Eq.(2):

$$J(\boldsymbol{x})=(\boldsymbol{Z}^{\text{meas}}-f(\boldsymbol{x}^{\text{est}}))^{\text{T}}\boldsymbol{R}^{-1}(\boldsymbol{Z}^{\text{meas}}-f(\boldsymbol{x}^{\text{est}})), \tag{2}$$

where $f(\boldsymbol{x}^{\text{est}})$ is the estimation of the measured values and $\boldsymbol{R}^{-1}$ is the inverse of the diagonal matrix of measurement variances.

By expanding Eq.(2) and calculating $\nabla J(\boldsymbol{x})=\boldsymbol{0}$, the WLS algorithm is given by

$$\boldsymbol{x}^{\text{est}}=(\boldsymbol{H}^{\text{T}}\boldsymbol{R}^{-1}\boldsymbol{H})^{-1}(\boldsymbol{H}^{\text{T}}\boldsymbol{R}^{-1}\boldsymbol{Z}^{\text{meas}}). \tag{3}$$

With Eq.(3), the voltages can be determined even though some measurements are lost. The errors introduced in the measurements are filtered in the WLS calculation. The most important advantage of this WLS algorithm is that due to the linearity of the relationship between WAMS measurement values and unknown voltages, an iterative calculation is not required. In other words, the state estimation can be finished quickly.

But the prerequisite of this linear weighted least squares (LWLS) state estimation is a full rank matrix $\boldsymbol{H}$, i.e.,

$$\text{rank}(\boldsymbol{H})=2n-1, \tag{4}$$

where n is the number of buses in the system. Otherwise, Eq.(3) will go singular.

Eq.(4) is the so-called 'numerical observability criterion'. In a sense, there is another observability, called 'topological observability' (Peng *et al*., 2006), which is defined as that all the buses in the power grid can be directly or indirectly measured by PMUs.

The above analysis shows that the guarantee of full observability is the foundation of LWLS.

PMU placement rules and the loss of observability

There are four rules for PMU placement (Baldwin and Mili, 1993):

Rule 1 Assign one direct voltage measurement to a bus where a PMU has been placed, including one current measurement to each branch connected to the bus itself.

Rule 2 Assign one indirect voltage measurement to each bus reached by another bus equipped with a PMU.

Rule 3 Assign one indirect current measurement to each branch connecting two buses where voltages are known. This allows interconnecting observed zones.

Rule 4 Assign one indirect current measurement to each branch where current can be indirectly calculated by Kirchhoff's current law (KCL). This rule

applies when the current balance at one bus is known, i.e., if the bus has no power injections (if $N-1$ currents incident to the bus are known, the last current can be computed by difference).

If all the buses in the power grid are assigned with direct or indirect voltage measurement, this PMU placement set is considered to be fully observable.

Due to the economic constraint, the number of PMUs is very limited, typically about 1/4~1/3 of the total buses in the power grid. As a result, the measurement redundancy of WAMS is much lower than that of SCADA. The topology change or PMU malfunction may break one of the above four rules and consequently make the WAMS lose its full observability. In a cascading failure, there are always more than one line tripping, which will make more buses become unobservable.

LINEAR INTERPOLATION METHOD

The linear interpolation method is briefly introduced here, and the error analysis of this method is also given.

Linear interpolation method

Once the WAMS loses its observability, cautions must be taken to restore the full observability. This is the remedial measure against cascading failures besides the redundant measurements of PMUs. Reynaldo (2001) proposed to use the linear interpolation method of neighboring measured voltage to estimate the voltages of unobservable buses.

First we simply introduce the linear interpolation method. Considering the case that one bus is unobservable (Fig.1), we can express the voltage of the unobservable bus X, $\dot{V}_{\mathrm{X}}$, in terms of the calculated voltages $\dot{V}_{\mathrm{C}}$ and $\dot{V}_{\mathrm{E}}$. Applying KCL to the unobservable bus X yields

$$0=\dot{V}_{\mathrm{X}}y_{\mathrm{XX}}+(\dot{V}_{\mathrm{X}}-\dot{V}_{\mathrm{C}})y_{\mathrm{CX}}+(\dot{V}_{\mathrm{X}}-\dot{V}_{\mathrm{E}})y_{\mathrm{EX}}, \quad (5)$$

where y_{CX} and y_{EX} are the complex admittances of the lines linking bus X to buses C and E respectively, and y_{XX} is the equivalent complex admittance of the power injection, which can be expressed in terms of bus real and complex power injection as shown in Eq.(6):

$$y_{\mathrm{XX}}=\frac{\dot{I}_{\mathrm{X}}}{\dot{V}_{\mathrm{X}}}=\frac{S_{\mathrm{X}}^{*}}{|\dot{V}_{\mathrm{X}}|^{2}}. \quad (6)$$

From Eq.(5), $\dot{V}_{\mathrm{X}}$ can be expressed in terms of $\dot{V}_{\mathrm{C}}$ and $\dot{V}_{\mathrm{E}}$:

$$\dot{V}_{\mathrm{X}}=\frac{y_{\mathrm{CX}}}{y_{\mathrm{XX}}+y_{\mathrm{CX}}+y_{\mathrm{EX}}}\dot{V}_{\mathrm{C}}+\frac{y_{\mathrm{EX}}}{y_{\mathrm{XX}}+y_{\mathrm{CX}}+y_{\mathrm{EX}}}\dot{V}_{\mathrm{E}}. \quad (7)$$

Similarly, for the two unobservable buses in Fig.2, the voltages $\dot{V}_{\mathrm{Y}}$ and $\dot{V}_{\mathrm{Z}}$ can be expressed in terms of known voltages $\dot{V}_{\mathrm{S}}$ and $\dot{V}_{\mathrm{T}}$ by applying KCL to buses Y and Z, respectively:

$$\begin{cases}0=\dot{V}_{\mathrm{Y}}y_{\mathrm{YY}}+(\dot{V}_{\mathrm{Y}}-\dot{V}_{\mathrm{S}})y_{\mathrm{SY}}+(\dot{V}_{\mathrm{Y}}-\dot{V}_{\mathrm{Z}})y_{\mathrm{ZY}},\\ 0=\dot{V}_{\mathrm{Z}}y_{\mathrm{ZZ}}+(\dot{V}_{\mathrm{Z}}-\dot{V}_{\mathrm{T}})y_{\mathrm{TZ}}+(\dot{V}_{\mathrm{Z}}-\dot{V}_{\mathrm{Y}})y_{\mathrm{ZY}},\end{cases} \quad (8)$$

where y_{YY} and y_{ZZ} are the complex load admittances of the unobservable buses Y and Z respectively, y_{SY} and y_{TZ} are the complex line admittances from buses Y and Z to buses S and T with known voltages respectively, and y_{ZY} is the complex admittance linking the unobservable buses.

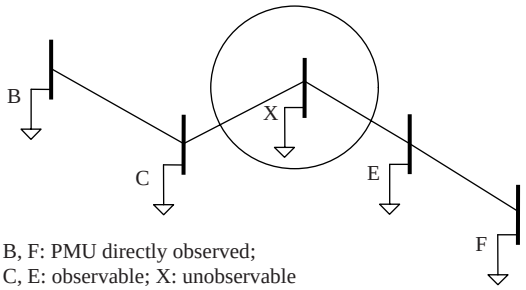

Fig.1 Illustration of one unobservable bus

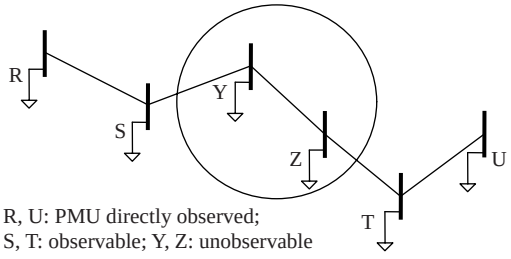

Fig.2 Illustration of two unobservable buses

Eqs.(9) and (10) can be obtained by solving Eq.(8):

$$\dot{V}_{\mathrm{Y}}=\frac{y_{\mathrm{SY}}}{Y_{\mathrm{Y}}-y_{\mathrm{ZY}}^2/Y_{\mathrm{Z}}}\dot{V}_{\mathrm{S}}+\frac{y_{\mathrm{ZY}}y_{\mathrm{TZ}}}{(Y_{\mathrm{Y}}-y_{\mathrm{ZY}}^2/Y_{\mathrm{Z}})Y_{\mathrm{Z}}}\dot{V}_{\mathrm{T}}, \quad (9)$$

$$\dot{V}_{\mathrm{Z}}=\frac{y_{\mathrm{SY}}y_{\mathrm{TZ}}}{(Y_{\mathrm{Z}}-y_{\mathrm{ZY}}^2/Y_{\mathrm{Y}})Y_{\mathrm{Y}}}\dot{V}_{\mathrm{S}}+\frac{y_{\mathrm{TZ}}}{Y_{\mathrm{Z}}-y_{\mathrm{ZY}}^2/Y_{\mathrm{Y}}}\dot{V}_{\mathrm{T}}, \quad (10)$$

where $Y_{\mathrm{Y}}=y_{\mathrm{SY}}+y_{\mathrm{ZY}}+y_{\mathrm{YY}}$, $Y_{\mathrm{Z}}=y_{\mathrm{TZ}}+y_{\mathrm{ZY}}+y_{\mathrm{ZZ}}$.

Error analysis of the linear interpolation method

This method has the following two drawbacks:

(1) It ignores the susceptance, which is comparatively large in long distance transmission lines. For WAMS, all transformers and transmission lines with voltage lower than 500 kV are considered as load. Hence the charging power should be treated as load. The load of a typical 500-kV substation in China is −2.6688−j0.3191 p.u., and the charging power of its neighboring transmission lines is −0.4027−j0.1448 p.u. The ignorance of charging power will cause 15.09% and 45.38% errors in the active and reactive load, respectively.

(2) It ignores the voltage characteristic of the load.

The static voltage characteristic of the load on an unobservable bus is described with the ZIP model (constant impedance, current, and PQ load) (Li *et al.*, 2007):

$$\begin{cases}P_{\mathrm{X}}=P_{\mathrm{X0}}[C_{P1}(U_{\mathrm{X}}/U_{\mathrm{X0}})^2+C_{P2}(U_{\mathrm{X}}/U_{\mathrm{X0}})+C_{P3}],\\ Q_{\mathrm{X}}=Q_{\mathrm{X0}}[C_{Q1}(U_{\mathrm{X}}/U_{\mathrm{X0}})^2+C_{Q2}(U_{\mathrm{X}}/U_{\mathrm{X0}})+C_{Q3}],\\ \text{s.t.}\ \ C_{P1}+C_{P2}+C_{P3}=1,\ \ C_{Q1}+C_{Q2}+C_{Q3}=1,\end{cases} \quad (11)$$

where C_{P1}, C_{P2} and C_{P3} are the percentages of constant impedance load, constant current load and constant power load respectively in active load; C_{Q1}, C_{Q2} and C_{Q3} are the percentages of constant impedance load, constant current load and constant power load respectively in reactive load; U_{X0} is the voltage magnitude of bus X at time t_0; U_{X} is the voltage magnitude of bus X at time t; P_{X0} and Q_{X0} are the active and reactive loads on bus X at time t_0, respectively; P_{X} and Q_{X} are the active and reactive loads on bus X at time t, respectively.

Considering the voltage characteristic of the load, we have

$$\begin{aligned}y_{\mathrm{XX}}&=\frac{S_{\mathrm{X}}^*}{|\dot{V}_{\mathrm{X}}|^2}=\frac{S_{\mathrm{X}}^*}{U_{\mathrm{X}}^2}\\ &=-\mathrm{conj}\left\{\frac{P_{\mathrm{X0}}[C_{P1}(U_{\mathrm{X}}/U_{\mathrm{X0}})^2+C_{P2}(U_{\mathrm{X}}/U_{\mathrm{X0}})+C_{P3}]}{U_{\mathrm{X}}^2}\right.\\ &\quad\left.+\mathrm{j}\frac{Q_{\mathrm{X0}}[C_{Q1}(U_{\mathrm{X}}/U_{\mathrm{X0}})^2+C_{Q2}(U_{\mathrm{X}}/U_{\mathrm{X0}})+C_{Q3}]}{U_{\mathrm{X}}^2}\right\}\\ &=-(C_1+C_2/U_{\mathrm{X}}+C_3/U_{\mathrm{X}}^2)+\mathrm{j}(C_4+C_5/U_{\mathrm{X}}+C_6/U_{\mathrm{X}}^2)\\ &=G_{\mathrm{XX}}+\mathrm{j}B_{\mathrm{XX}},\end{aligned} \quad (12)$$

where $C_i\geq 0$, i=1, 2, …, 6.

The tripping of lines usually results in the transfer of power to the neighboring lines, which will consequently reduce the magnitudes of the neighboring bus voltages. The post-fault bus voltage magnitude is therefore supposed to be lower than that before the fault, i.e.,

$$U_{\mathrm{X\_before}}>U_{\mathrm{X\_after}}. \quad (13)$$

With both Eqs.(12) and (13), we have

$$\begin{cases}G_{\mathrm{XX\_before}}>G_{\mathrm{XX\_after}},\\ B_{\mathrm{XX\_before}}<B_{\mathrm{XX\_after}}.\end{cases} \quad (14)$$

Due to the similarity between the two parts of Eq.(7), only the analysis of the first part is given here:

$$\begin{aligned}&\frac{y_{\mathrm{CX}}}{y_{\mathrm{XX}}+y_{\mathrm{CX}}+y_{\mathrm{EX}}}\dot{V}_{\mathrm{C}}\\ &=\frac{y_{\mathrm{CX}}}{(G_{\mathrm{XX}}+G_{\mathrm{CX}}+G_{\mathrm{EX}})+\mathrm{j}(B_{\mathrm{XX}}+B_{\mathrm{CX}}+B_{\mathrm{EX}})}\dot{V}_{\mathrm{C}}\\ &=\frac{y_{\mathrm{CX}}\dot{V}_{\mathrm{C}}}{\sqrt{(G_{\mathrm{XX}}+G_{\mathrm{CX}}+G_{\mathrm{EX}})^2+(B_{\mathrm{XX}}+B_{\mathrm{CX}}+B_{\mathrm{EX}})^2}\,\mathrm{e}^{\mathrm{j}\theta}},\end{aligned} \quad (15)$$

where $\theta=\arctan\dfrac{B_{\mathrm{XX}}+B_{\mathrm{CX}}+B_{\mathrm{EX}}}{G_{\mathrm{XX}}+G_{\mathrm{CX}}+G_{\mathrm{EX}}}$.

With Eqs.(14) and (15), it is obvious that the estimated voltage angle is larger than the actual one when the voltage magnitude drops due to the opposite variation tendency of G_{XX} and B_{XX}. Due to the same reason, the difference between the estimated and actual voltage magnitudes is alleviated.

DYNAMIC VOLTAGE PHASOR TRACING METHOD

In this section, we present the dynamic voltage phasor tracing method and its flowchart.

Dynamic tracing method

The principle of the dynamic voltage phasor tracing method is illustrated in case of two unobservable buses, as shown in Fig.2. By considering the voltage characteristic of the load, the conjugation of the injection power on buses Y and Z can be expressed in the ZIP model as

$$S_{\mathrm{Y}}^{*}=-\mathrm{conj}\left\{P_{\mathrm{Y0}}[C_{P1}(U_{\mathrm{Y}}/U_{\mathrm{Y0}})^{2}+C_{P2}(U_{\mathrm{Y}}/U_{\mathrm{Y0}})+C_{P3}]+\mathrm{j}Q_{\mathrm{Y0}}[C_{Q1}(U_{\mathrm{Y}}/U_{\mathrm{Y0}})^{2}+C_{Q2}(U_{\mathrm{Y}}/U_{\mathrm{Y0}})+C_{Q3}]\right\}, \tag{16}$$

$$S_{\mathrm{Z}}^{*}=-\mathrm{conj}\left\{P_{\mathrm{Z0}}[C_{P1}(U_{\mathrm{Z}}/U_{\mathrm{Z0}})^{2}+C_{P2}(U_{\mathrm{Z}}/U_{\mathrm{Z0}})+C_{P3}]+\mathrm{j}Q_{\mathrm{Z0}}[C_{Q1}(U_{\mathrm{Z}}/U_{\mathrm{Z0}})^{2}+C_{Q2}(U_{\mathrm{Z}}/U_{\mathrm{Z0}})+C_{Q3}]\right\}. \tag{17}$$

The SCADA system gathers and stores the information on the magnitude of bus voltage, active power, and reactive power on the transmission line. The parameters of the ZIP model can be estimated by the least square method or recursive least square method (Milosevic and Miroslavca, 2003) with SCADA data. In this study, we simply assume that the parameters of the ZIP model, with certain errors, have already been identified.

The impact of the susceptance is also taken into consideration, and thus the self-admittance is modified as follows:

$$y_{\mathrm{YY}}=\frac{S_{\mathrm{Y}}^{*}}{\left|V_{\mathrm{Y}}\right|^{2}}+\mathrm{j}\frac{B_{\mathrm{SY}}+B_{\mathrm{YZ}}}{2}=\frac{S_{\mathrm{Y}}^{*}}{U_{\mathrm{Y}}^{2}}+\mathrm{j}\frac{B_{\mathrm{SY}}+B_{\mathrm{YZ}}}{2}, \tag{18}$$

$$y_{\mathrm{ZZ}}=\frac{S_{\mathrm{Z}}^{*}}{\left|V_{\mathrm{Z}}\right|^{2}}+\mathrm{j}\frac{B_{\mathrm{YZ}}+B_{\mathrm{ZT}}}{2}=\frac{S_{\mathrm{Z}}^{*}}{U_{\mathrm{Z}}^{2}}+\mathrm{j}\frac{B_{\mathrm{YZ}}+B_{\mathrm{ZT}}}{2}, \tag{19}$$

where B_{SY}, B_{YZ}, and B_{ZT} are the susceptances of lines (S, Y), (Y, Z), and (Z, T), respectively.

Since the measurement precision of the voltage magnitude is higher than that of the voltage angle by PMUs (Yang *et al*., 2003), the voltage magnitude is adopted as the independent variable of the nonlinear equations, as shown in Eq.(20):

$$\begin{cases}U_{\mathrm{Y}}=\left|\dfrac{y_{\mathrm{SY}}}{Y_{\mathrm{Y}}-y_{\mathrm{ZY}}^{2}/Y_{\mathrm{Z}}}\dot{V}_{\mathrm{S}}+\dfrac{y_{\mathrm{ZY}}y_{\mathrm{TZ}}}{(Y_{\mathrm{Y}}-y_{\mathrm{ZY}}^{2}/Y_{\mathrm{Z}})Y_{\mathrm{Z}}}\dot{V}_{\mathrm{T}}\right|,\\ U_{\mathrm{Z}}=\left|\dfrac{y_{\mathrm{SY}}y_{\mathrm{TZ}}}{(Y_{\mathrm{Z}}-y_{\mathrm{ZY}}^{2}/Y_{\mathrm{Y}})Y_{\mathrm{Y}}}\dot{V}_{\mathrm{S}}+\dfrac{y_{\mathrm{TZ}}}{Y_{\mathrm{Z}}-y_{\mathrm{ZY}}^{2}/Y_{\mathrm{Y}}}\dot{V}_{\mathrm{T}}\right|,\end{cases} \tag{20}$$

where $Y_{\mathrm{Y}}=y_{\mathrm{SY}}+y_{\mathrm{ZY}}+y_{\mathrm{YY}}$, $Y_{\mathrm{Z}}=y_{\mathrm{TZ}}+y_{\mathrm{ZY}}+y_{\mathrm{ZZ}}$.

Eq.(20) can be expressed in the form of functions as

$$\begin{cases}U_{\mathrm{Y}}=f_{\mathrm{Y}}(U_{\mathrm{Y}},U_{\mathrm{Z}}),\\ U_{\mathrm{Z}}=f_{\mathrm{Z}}(U_{\mathrm{Y}},U_{\mathrm{Z}}).\end{cases} \tag{21}$$

To solve these nonlinear equations, the Gauss-Seidel algorithm is employed. Once the voltage magnitude of an unobservable bus is found, the voltage phasor of unobservable buses can be calculated by

$$\dot{V}_{\mathrm{Y}}=\frac{y_{\mathrm{SY}}}{Y_{\mathrm{Y}}-y_{\mathrm{ZY}}^{2}/Y_{\mathrm{Z}}}\dot{V}_{\mathrm{S}}+\frac{y_{\mathrm{ZY}}y_{\mathrm{TZ}}}{(Y_{\mathrm{Y}}-y_{\mathrm{ZY}}^{2}/Y_{\mathrm{Z}})Y_{\mathrm{Z}}}\dot{V}_{\mathrm{T}}, \tag{22}$$

$$\dot{V}_{\mathrm{Z}}=\frac{y_{\mathrm{SY}}y_{\mathrm{TZ}}}{(Y_{\mathrm{Z}}-y_{\mathrm{ZY}}^{2}/Y_{\mathrm{Y}})Y_{\mathrm{Y}}}\dot{V}_{\mathrm{S}}+\frac{y_{\mathrm{TZ}}}{Y_{\mathrm{Z}}-y_{\mathrm{ZY}}^{2}/Y_{\mathrm{Y}}}\dot{V}_{\mathrm{T}}. \tag{23}$$

Flowchart of the dynamic voltage phasor tracing method

The function of this new nonlinear estimation is to restore the observability of the unobservable bus voltage. In order to improve the robustness, the linear interpolation method is employed when the Gauss-Seidel method fails to solve the equations within a certain number of iterations. As shown in Fig.3, the dynamic voltage phasor tracing method can be integrated as an accessory model to the existing linear state estimator, and thus no program modification is needed.

CASE STUDY

In this section, we provide some numerical examples to illustrate the performance of the nonlinear dynamic voltage phasor tracing method.

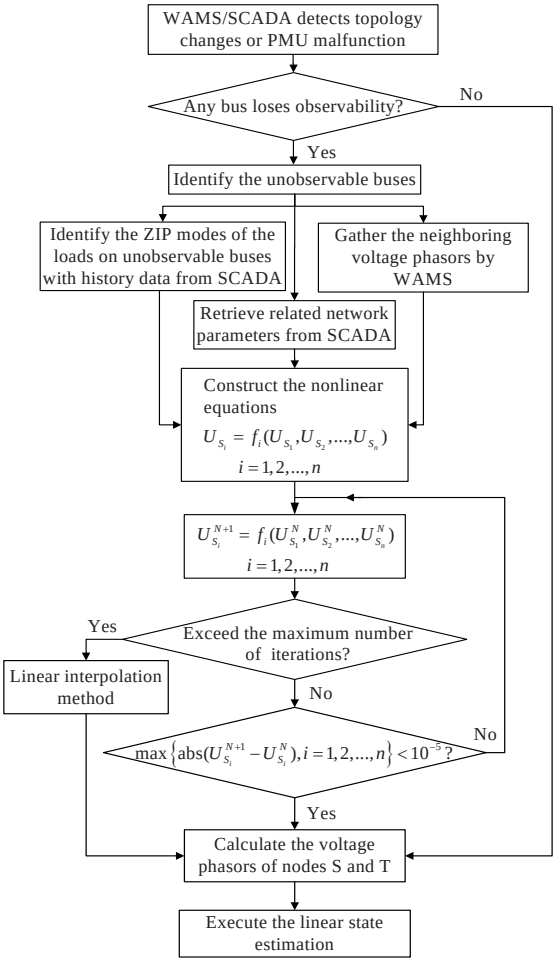

Fig.3 Flowchart of the dynamic voltage phasor tracing method

Impact of the cascading failure and PMU malfunction on the observability of WAMS

In order to gain an insight into the impact of a cascading failure and PMU malfunction on the observability of WAMS, the IEEE 39-bus system was employed. As shown in Fig.4, the PMU placement set was generated by the simulating annealing method (Baldwin and Mili, 1993). Six depth-2 and depth-3 cascading failures are listed in Table 1. These cascading failures make the WAMS lose its full observability. Under the worst condition, three buses will become unobservable.

The impact of PMU malfunction was also studied by removing one PMU each time and recalculating the observable area. The simulation results are listed in Table 2. Accordingly, the loss of any PMU will cause the WAMS to lose its full observability, and the loss of the PMU on bus 6 will induce seven unobservable buses.

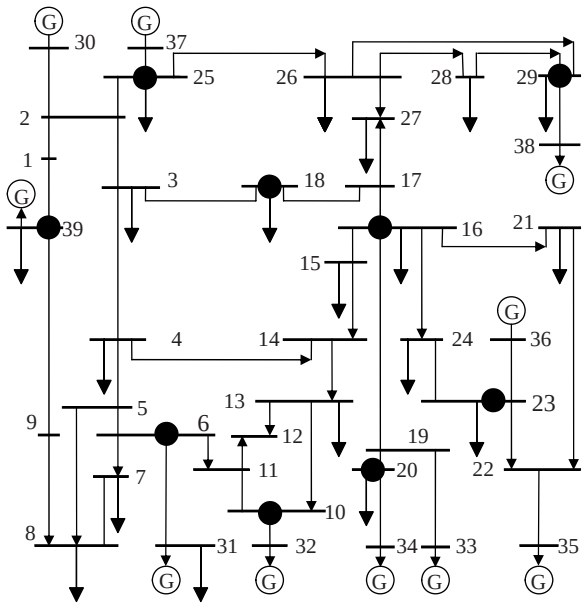

Fig.4 The PMU placement set of the IEEE 39-bus system generated by the simulating annealing method

Table 1 The unobservability caused by a cascading failure

Tripped lines	Unobservable bus No.
(12, 13), (5, 6)	5
(6, 7), (5, 8)	7
(6, 7), (5, 6)	5, 7
(7, 8), (5, 6), (4, 14)	4, 5
(7, 8), (5, 8), (1, 39)	1, 30
(6, 7), (5, 6), (4, 14)	4, 5, 7

Table 2 The unobservability caused by PMU malfunction

Malfunction PMU No.	Unobservable bus No.
6	4, 5, 6, 7, 12, 14, 31
10	10, 12, 13, 14, 32
16	16, 21, 27, 33, 35
18	3, 18, 27, 30
20	20, 33, 34
23	22, 23, 35, 36
25	25, 30, 37
29	28, 29, 38
30	1, 9, 30, 39

The above analysis illustrates that the WAMS is vulnerable to the cascading failure and PMU malfunction. That is why countermeasures are eagerly needed to restore the full observability the moment it is lost.

Estimation of the voltage of the unobservable bus

Case 1: one bus is unobservable.

PAST^{TM} 1.3.3 was adopted to carry out time domain simulation. Line (5, 6) was tripped at 1.25 s and the measured voltages on buses 4 and 8 were used to estimate the unobservable voltage on bus 5. A load with P+jQ=4+j2 (p.u.) was added to bus 5. All loads in the test system were modeled in the ZIP load model and their parameters were set as follows:

$$C_{P1}=C_{Q1}=5\%,\ C_{P2}=C_{Q2}=5\%,\ C_{P3}=C_{Q3}=90\%. \quad (24)$$

By considering the errors introduced in the identification of load parameters, the identified load parameters were supposed to have about 10% errors:

$$C_{P1}=C_{Q1}=8\%,\ C_{P2}=C_{Q2}=11\%,\ C_{P3}=C_{Q3}=81\%. \quad (25)$$

The convergence error of the Gauss-Seidel method was set to 10^{-5}.

In order to estimate the efficiency of this dynamic tracing method, the linear interpolation method proposed in (Reynaldo, 2001) was also carried out for comparison. Two new indexes, max error (ME) and max error percentage (MEP), were defined as follows:

$$ME=\max\{|V_i^{\text{act}}-V_i^{\text{est}}|,\ i=1, 2, \ldots, k\}, \quad (26)$$

$$MEP=\max\{|V_i^{\text{act}}-V_i^{\text{est}}|/|V_i^{\text{act}}|\times 100\%,\ i=1, 2, \ldots, k\}, \quad (27)$$

where k is the times of data sampling, V_i^{act} is the actual value, and V_i^{est} is the estimated value.

Simulation results are shown in Fig.5, and the error analysis results are listed in Table 3. From the results, one can learn that the relative power angle between two buses of one transmission line is usually very small, typically no larger than 20°, which is about 0.174 rad (Han, 1993). First, the linear interpolation method was used to estimate the voltage phasor of bus 5. The MEP of the relative power angle of lines (4, 5) and line (5, 8) are 19.11% and 13.82%, respectively. In this case, the error, 0.0045 rad, is very notable. At the same time, the MEP of the voltage magnitude is only about 0.3%. The adoption of the dynamic tracing method reduces the MEP of the relative power angle to 0.76% and the MEP of the voltage magnitude to 0.07%. As a result, the dynamic voltage phasor tracing method can greatly improve the estimation accuracy of the relative power angle, but the effect is not so significant in improving the accuracy of the voltage magnitude estimation.

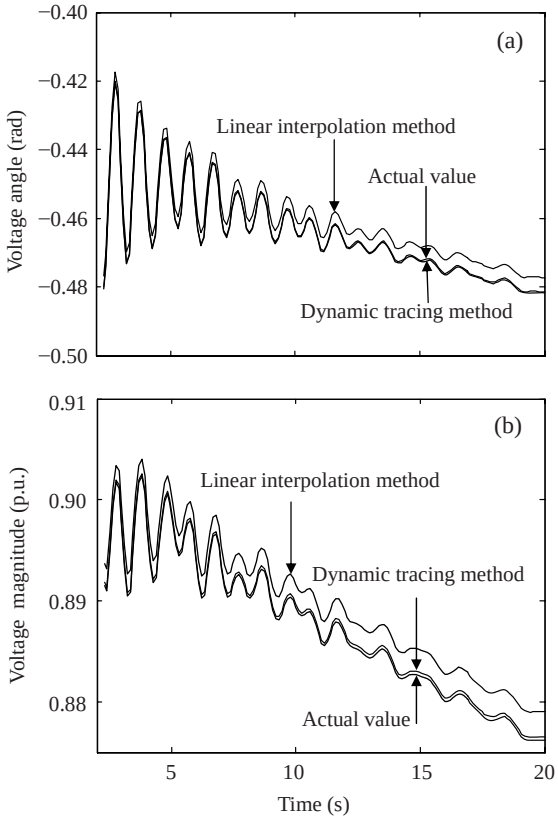

Fig.5 Voltage angle (a) and voltage magnitude (b) of bus 5

Table 3 Results comparison when one bus is unobservable

Data type	*ME*		*MEP* (%)	
	LI	DT	LI	DT
$\Delta\delta$ between buses 4 and 5	4.5×10^{-3} rad	2.494×10^{-4} rad	19.11	1.05
$\Delta\delta$ between buses 5 and 8	4.5×10^{-3} rad	2.494×10^{-4} rad	13.82	0.76
Voltage magnitude of bus 5	2.8×10^{-3} p.u.	6.643×10^{-4} p.u.	0.29	0.07

LI: linear interpolation method; DT: dynamic tracing method.
$\Delta\delta$: relative angle between two buses

Case 2: two buses are unobservable.

In this case, line (3, 4) was tripped at 1.25 s and measured voltages on buses 4 and 17 were used to estimate the unobservable voltages on buses 3 and 18. No load was added to bus 5. The load parameters and identified load parameters were the same as those in Case 1.

The simulation results are shown in Figs.6 and 7, and the error analysis results are given in Table 4. With the linear interpolation method, the ME of the relative power angle is 0.0093 rad, and the MEP of the voltage magnitude is about 0.30%. The MEPs of the relative power angles are 22.78%, 51.60% and 13.96%. According to the results, the actual values were badly polluted by errors and the interaction between errors of the estimated voltage phasors of unobservable buses severely magnified the estimation errors. As a result, much more serious errors can be expected by the linear interpolation method if there are more unobservable buses. However, the error caused by the dynamic tracing method is much smaller. With the dynamic voltage phasor tracing method the MEP of the relative power angle can be reduced to 4.60%, while the ME of the voltage magnitude is only a bit smaller than that by the linear estimation method. This simulation justifies that the dynamic tracing method can greatly improve the estimation accuracy of the relative power angle.

Table 4 Results comparison when two buses are unobservable

Data type	*ME*		*MEP* (%)	
	LI	DT	LI	DT
$\Delta\delta$ between buses 3 and 4	9.3×10^{-3} rad	6.542×10^{-4} rad	22.78	2.03
$\Delta\delta$ between buses 3 and 18	9.3×10^{-3} rad	6.542×10^{-4} rad	51.60	4.60
$\Delta\delta$ between buses 17 and 18	6.7×10^{-3} rad	6.026×10^{-4} rad	13.96	1.24
Voltage magnitude of bus 3	9.3×10^{-4} p.u.	2.298×10^{-4} p.u.	0.09	0.02
Voltage magnitude of bus 18	1.3×10^{-3} p.u.	2.964×10^{-4} p.u.	0.14	0.30

LI: linear interpolation method; DT: dynamic tracing method.
$\Delta\delta$: relative angle between two buses

In these two cases, the solution process converges rapidly, and it needs only four iterations at most, which indicates that the dynamic voltage phasor tracing method has an impressive calculation speed as well as the potential for online applications.

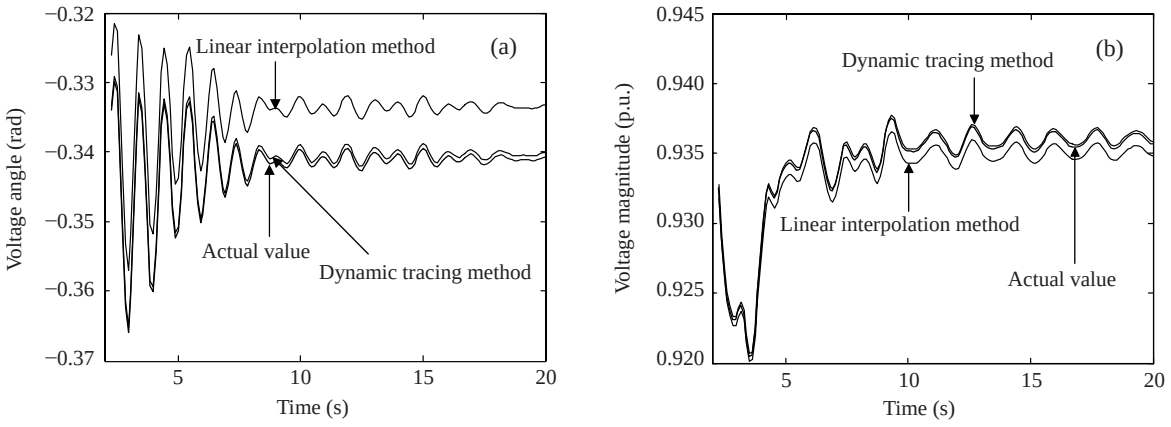

Fig.6 Voltage angle (a) and voltage magnitude (b) of bus 3

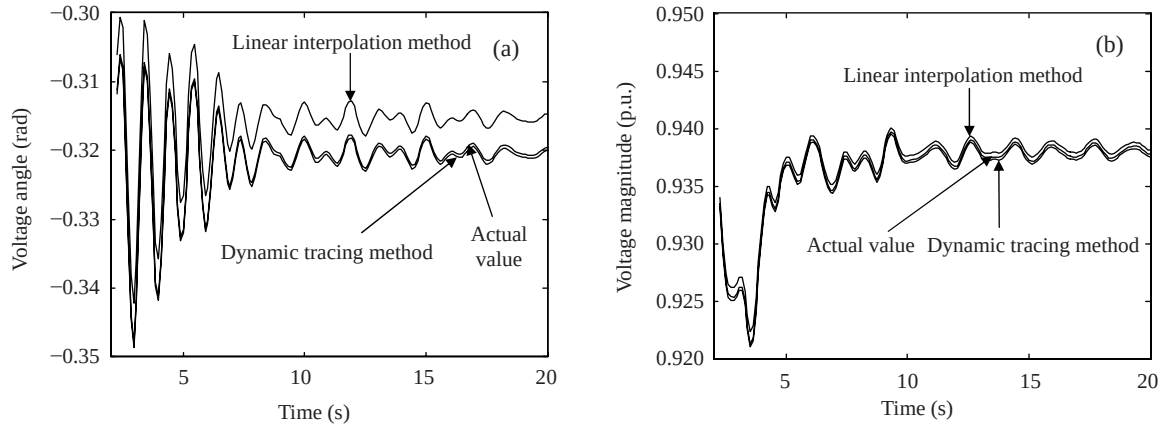

Fig.7 Voltage angle (a) and voltage magnitude (b) of bus 18

Impact of load model parameter perturbation on estimation accuracy

The composition of the ZIP model varies throughout the day. As a result, the impact of the load model parameter perturbation on estimation accuracy is specially studied here. The results are given in Table 5. Comparing the cases in Tables 3 and 5, we can find that C_{P1} has more effect on estimation accuracy than C_{P2}, and that the estimation accuracy is still higher than that in the linear interpolation method when the composition of load is changed. In comparison with the active load model parameter perturbation, the reactive load model parameter perturbation has much lighter impact.

Table 5 Impact of load model parameter perturbation on estimation accuracy

Parameter	Actual value (%)	Estimated value (%)			
		Case 1	Case 2	Case 3	Case 4
C_{P1}	5	25	5	5	5
C_{P2}	5	5	25	5	5
C_{P3}	90	70	70	90	90
C_{Q1}	5	5	5	25	5
C_{Q2}	5	5	5	5	25
C_{Q3}	90	90	90	70	70
MEP of the voltage of bus 5		4.80	2.70	0.36	0.30
MEP of the angle between buses 4 and 5		3.40	2.00	0.26	0.21
MEP of the angle between buses 5 and 8		0.02	0.02	0.09	0.05

CONCLUSION

A WAMS/SCADA mixed dynamic voltage phasor tracing method is proposed to dynamically estimate the voltage phasor of unobservable buses. Through theoretical analysis and simulation, two conclusions are obtained: (1) This method greatly improves the estimation accuracy of the relative power angle, but not too much on the voltage magnitude estimation; (2) This method provides a novel research prospect for improving the robustness of the WAMS against cascading failures and PMU malfunction.

References

Baldwin, T.L., Mili, L., 1993. Power system observability with minimal phasor measurement placement. *IEEE Trans. Power Syst.*, **8**(2):707-715. [doi:10.1109/59.260810]

Chaudhuri, B., Majumder, R., Pal, B., 2004. Wide-area measurement-based stabilizing control of power system considering signal transmission delay. *IEEE Trans. Power Syst.*, **19**(4):1971-1979. [doi:10.1109/TPWRS.2004.835669]

Chen, J., Abur, A., 2006. Placement of PMUs to enable bad data detection in state estimation. *IEEE Trans. Power Syst.*, **21**(4):1608-1615. [doi:10.1109/TPWRS.2006.881149]

Han, Z.X., 1993. Power System Analysis. Zhejiang University Press, Hangzhou, China (in Chinese).

Huang, K.S., Wu, Q.H., Turner, D.R., 2002. Effective identification of induction motor parameters based on fewer measurements. *IEEE Trans. Energy Conv.*, **17**(1):55-60. [doi:10.1109/60.986437]

Li, Y., Chiang, H.D., Choi, B.K., Chen, Y.T., Huang, D.H., Lauby, M.G., 2007. Representative static load models for transient stability analysis: development and examination. *IET Gener. Trans. Distrib.*, **1**(3):422-431. [doi:10.1049/iet-gtd:20060044]

Milosevic, B., Miroslavca, B., 2003. Voltage-stability protection and control using a wide-area network of phasor measurement. *IEEE Trans. Power Syst.*, **18**(1):121-127. [doi:10.1109/TPWRS.2002.805018]

Okou, F., Dessaint, L., Akhrif, O., 2005. Power systems stability enhancement using a wide-area signals based hierarchical controller. *IEEE Trans. Power Syst.*, **20**(3):1465-1477. [doi:10.1109/TPWRS.2005.852056]

Peng, J.N., Sun, Y.Z., Wang, H.F., 2006. Optimal PMU placement for full network observability using tabu search algorithm. *Int. J. Electr. Power Energy Syst.*, **28**(4):223-231. [doi:10.1016/j.ijepes.2005.05.005]

Quintero, J., Venkatasubramanian, V., 2005. A Real-time Wide-area Control Framework for Mitigating Small-signal Instability in Large Electric Power Systems. Proc. 38th Hawaii Int. Conf. on System Sciences, p.1-10. [doi:10.1109/HICSS.2005.43]

Rehtanz, C., Bertsch, J., 2002. Wide Area Measurement and Protection System for Emergency Voltage Stability Control. Proc. Power Engineering Society Winter Meeting, p.842-847. [doi:10.1109/PESW.2002.985124]

Reynaldo, F.N., 2001. State Estimation and Voltage Security Monitoring Using Synchronized Phasor Measurements. PhD Thesis, Virginia Polytechnic Institute and State University, Blacksburg, Virginia, USA.

Yang, G.Y., Jiang, D.Z., Qiu, J.J., 2003. Synchronous measurement precision of phasor measurement unit. *Autom. Electr. Power Syst.*, **27**(14):57-61.

Zima, M., Krause, T., Andersson, G., 2003. Evaluation of System Protection Schemes, Wide Area Monitoring and Control Systems. Proc. 6th Int. Conf. on Advances in Power System Control, Operation and Management, **2**:754-759. [doi:10.1049/cp:20030680]